Hindawi
Advances in Civil Engineering
Volume 2019, Article ID 9816067, 11 pages
https://doi.org/10.1155/2019/9816067

Research Article

Crack Initiation, Propagation, and Coalescence Experiments in Sandstone Brazilian Disks Containing Pre-Existing Flaws

Shijun Zhao[1,2] **Qing Zhang**[1] **and Limin Liu**[3]

[1]*College of Mechanics and Materials, Hohai University, Nanjing 211100, China*
[2]*Department of Mechanical and Materials Engineering, University of Nebraska-Lincoln, Lincoln, NE 68588, USA*
[3]*College of Mining and Safety Engineering, Shandong University of Science and Technology, Qingdao 266590, China*

Correspondence should be addressed to Qing Zhang; lxzhangqing@hhu.edu.cn

Received 9 October 2018; Revised 7 November 2018; Accepted 11 December 2018; Published 22 January 2019

Academic Editor: Qingliang Yu

This study aims to investigate the fracture behaviors of cracks and crack systems in Brazilian disk (BD) sandstone specimens under compressive line loading. We conduct a series of rock fracture experiments to investigate crack initiation, propagation, and coalescence in samples with one or more pre-existing flaws under radial compressive stress. The displacements and failure loads of the tested specimens are measured. Experimental results show that there are two main types of cracks growing from the pre-existing flaws: wing cracks and secondary cracks. Both initiate mostly from the tips of the pre-existing flaws and propagate in a stable manner. The results reveal that wing cracks appear first and propagate toward the loading direction. Secondary cracks can form in some multiple pre-cracked cases after wing cracks are already present. We also provide a characterization of the observed crack propagation paths and patterns and discuss the influence of pre-existing crack or crack systems. The results help in investigating the failure mechanisms and mechanical properties of rock or rock-like materials.

1. Introduction

In general, rock mass is a natural formation of mineral aggregates which may contain voids, cracks, and other defects at different scales. This makes rocks' internal structure discontinuous [1–3], as shown in Figure 1. The presence of pre-existing defects may reduce the fracture toughness of rock mass, and such defects are also a source of initiation of new fracture lines or cracks. Crack growth and catastrophic failures initiated from the pre-existing defects subjected to multiaxial loads is one of the main concerns for geotechnical engineers and designers of underground structures. Under external and internal pressures, cracks can initiate and propagate from those pre-existing cracks or pores and then coalesce into macrofailure of the rock structure.

Because of the difficulties of in-situ tests, the laboratory experiment is an important and effective research method to investigate rock failure modes and fracture mechanisms, in the presence of pre-existing defects that can be easily inserted into the samples. Over the last few decades, many experiments have been devoted to using semi-circular core in three-point bending (SCB) specimen [4], Brazilian disk (BD) specimen with chevron flaws or other pre-existing flaws [5], radial cracked ring (RCR) specimen [6], and modified ring (MR) specimen [7] to investigate rock fracture toughness and crack propagation. Brace and Bombolakis [8] conducted an experimental study on fracture mechanisms in rock material, and it is considered one of the earliest studies in this field. Then, the extensive studies have been performed on cracking failure processes evolution from pre-existing discontinuities that emerged in brittle materials. And a series of fracture experimental tests were conducted to study crack initiation, propagation, and coalescence under compressive diametric or cyclic uniaxial compression loading using pre-cracked specimens or intermittently joint rock models [9–16]. The crack propagation patterns usually obtained in previous studies of brittle material contain pre-existing flaws

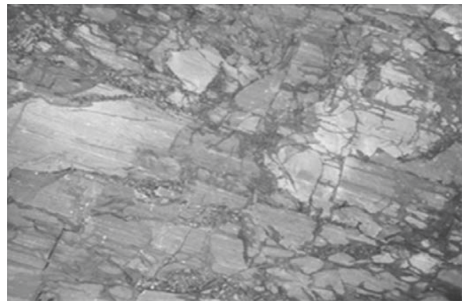

Figure 1: Schematic view of pre-existing defects in the natural rock mass.

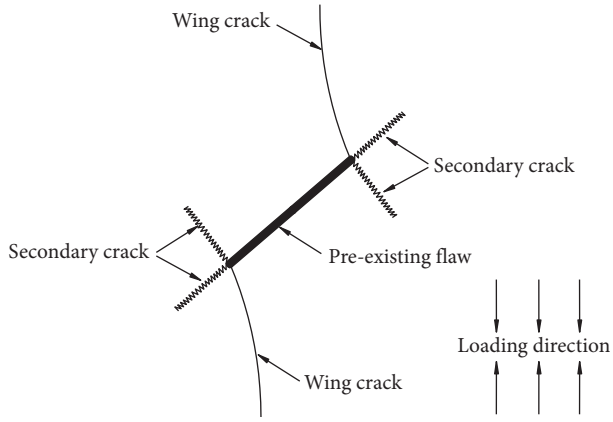

Figure 2: Simplified crack patterns in pre-cracked specimens of rock-like materials under uniaxial compression [9].

under uniaxial compression loading, as shown in Figure 2. Two types of cracks were observed: wing cracks and secondary cracks [17–20]. Based on different experiment conditions (such as the type of specimen, specimen size, pre-existing flaws geometry, and load arrangements), the researchers observed common crack characteristics: wing cracks come into being first, which are tensile cracks and they mostly initiate from the tips of the pre-existing flaws at an angle and then propagate to be parallel to the compressive direction. Secondary cracks are usually shear cracks that appear later than wing cracks. Those researchers believe that cracks coalesce on account of the development of shear cracks. Wong and Einstein [21, 22] studied the systematic evaluation of cracking behaviors in specimens with pre-existing flaws and observed the cracking mechanism with enough details under uniaxial compression using the high-speed camera. Figure 3 shows the category of coalescence patterns and seven crack types with different trajectories and initiation mechanism. Other researchers found cracks coalescence in the linkage areas of the pre-existing flaws, which is caused by the secondary cracks or the combined effects of wing cracks and secondary cracks. This can better illustrate the damage processes [23–33].

However, because of the complexity of natural rock mass, researchers usually used artificial materials such as resin, cement mortar, organic glass, or gypsum, which cannot reveal the fracture mechanisms and mechanical properties effectively. Moreover, the experimental studies about pre-existing crack systems in natural brittle sandstone material from deeper underground are still poorly. Crack initiation and propagation, especially coalescence, is dependent on the types of pre-existing flaws. Some pre-existing flaws may play a role in preventing cracks' propagation and coalescence as barriers. So, the crack propagation paths and load-carrying ability in practical applications can be significantly affected by the cracked flaw forms and types of conducted loading [34, 35]. To investigate crack propagation and crack coalescence in linkage areas, we develop pre-cracked specimens with different inclination angles and new types of specimens with pre-cracked crack systems. In this paper, the term "flaws" is used to describe the artificially created single crack or crack systems. The new types of crack systems consist of the forward echelon cracks system, inverse echelon crack system, two parallel cracks, three parallel cracks, and crack system with barrier cracks. The geometries of those pre-cracked flaws are expected to improve the understanding of fracture mechanisms of underground sandstone. Loads and displacements are recorded for all specimens during the whole breakage process. In addition, the load-displacement curves are shown to discuss the process of the tested specimens.

Therefore, the motivation for this work will focus on two points: (1) investigating the effects of pre-existing flaws on the cracking behaviors and the crack coalescence patterns in sandstone specimens containing different types of pre-

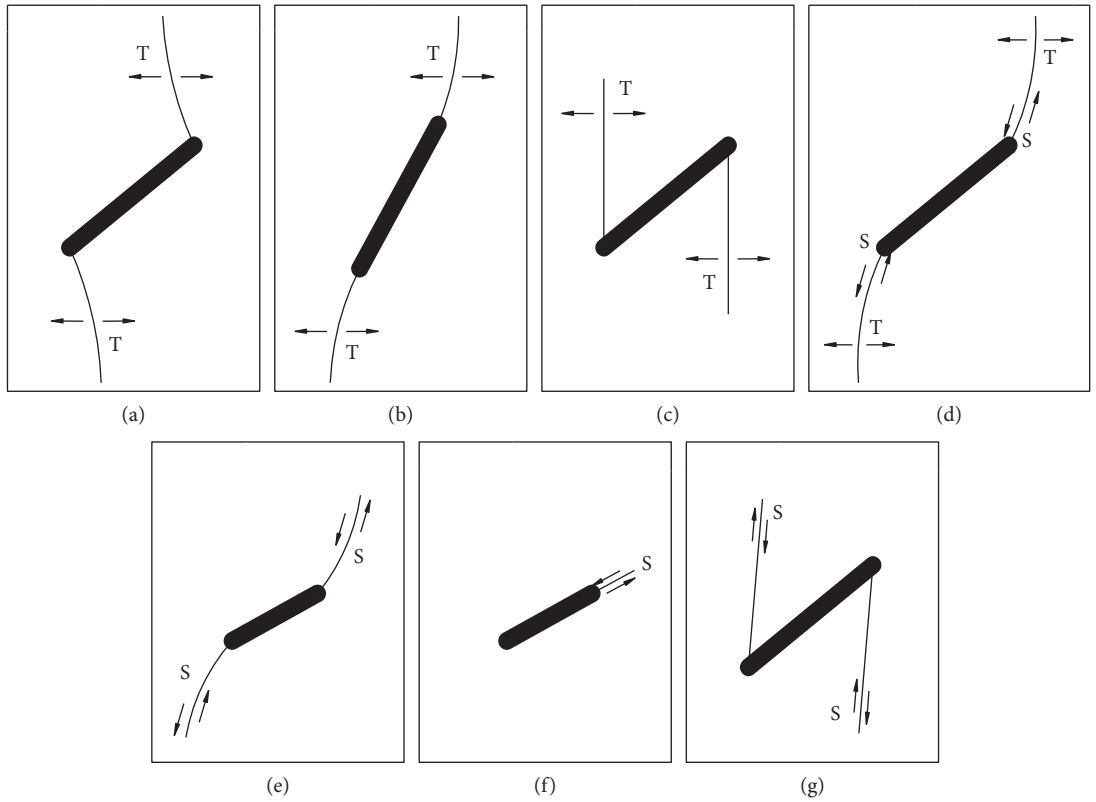

Figure 3: Various crack types initiated from the pre-existing flaw identified in the present studies (T = tensile cracking opening; S = shearing displacement) [21, 22]. (a–c) Tensile crack; (d) mixed tensile shear crack; (e–g) shear crack.

existing flaws and (2) characterizing and analyzing the crack initiation, propagation, and coalescence patterns from pre-existing flaws. This paper is organized as follows. In Section 2, the preparation of disk specimens and the experimental procedure are introduced. The experimental results are discussed in Sections 3 and 4. Finally, in Section 5, we draw some conclusions.

2. Preparation of Disk Specimens and Experimental Procedure

To study the fracture behavior of sandstone BD specimens, we cut specimens with pre-existing different inclination angles of crack and different types of the crack systems and tested them under compressive line loading. The sandstone is from about 900-meter depth underground strata in Juye Coalfield, Shandong Province, China.

2.1. Preparation of Specimens. The sandstone samples were excavated by geologic drilling from Juye Coalfield, whose Cenozoic formation is very thick. The average thickness of strata in the fourth system is 158.43 m, the average thickness of the upper tertiary strata is 497.01 m, and the thickness of the new boundary layer is 530~720 m, mainly composed of clay, sandy clay, sand, fine sand, and gravel. Main coal seam roof and floor sandstone thickness is 4.80~75.65 m, mainly composed of fine sandstone, local sandstone, and siltstone. The preparation of tested specimens for pre-cracked flaw procedures is explained as follows.

For manufacturing the test specimens, the whole tests used five samples and each one was cored into 30~50 cm long, with the diameter $D = 62$ mm cylindrical columns in the construction site. In order to avoid being influenced by surroundings, the surface of the samples was wrapped in a multilayer food preservation film after being removed from the formation. The specimens were cut into Brazilian disk shape, with a size of $\Phi\ 62 \times 30$ mm. The pre-existing flaws were created by high-speed water jet cutting machine. Figure 4 shows the pre-existing flaws preparation setup for tested specimens. The pre-existing flaws thickness is 30 mm. The flaw length, $2b$, is equal to 20 mm and the pre-existing flaws width is 1 mm. The radius and thickness of the tested BD specimens are $R = 31$ mm and $H = 30$ mm. Crack length ratio is an important parameter for the pattern, trajectory, and the number of fractures; in this work, the ratio b/R is 0.32.

Various Brazilian tests were conducted on BD specimens containing a single crack and different types of crack systems. Figure 5 shows geometries of pre-cracked specimens; the inclination angle (angle with the horizontal, β) varies from 0° to 90° at 15° interval. Furthermore, Figure 6 shows a schematic view of BD specimens containing different types of pre-existing crack systems. Finally, a total number of 31 pre-cracked specimens were tested, with two or three specimens at each inclination angles: $\beta = 0°$, 15°, 30°, 45°, 60°, 75°, and 90°. Two or three specimens at each type of crack

Figure 4: Pre-existing flaws preparation in sandstone BD specimens using a water jet cutting machine.

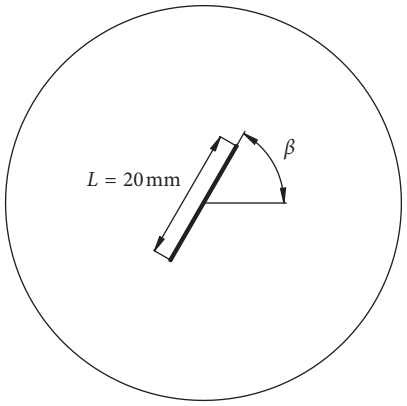

Figure 5: Geometry of pre-cracked specimens with different inclination angles: $\beta = 0$, 15°, 30°, 45°, 60°, 75°, and 90°.

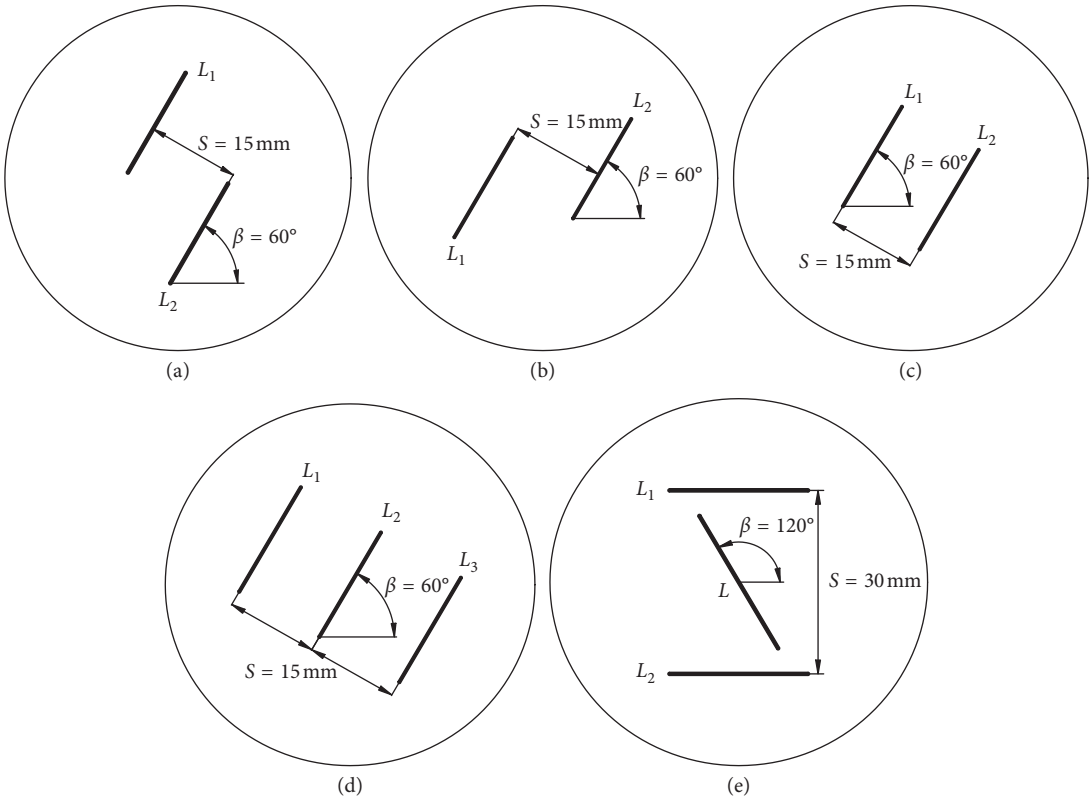

Figure 6: Geometries of different types of crack systems: (a) forward echelon crack system, (b) inverse echelon crack system, (c) two parallel cracks, (d) three parallel cracks, and (e) crack system with barrier cracks.

systems contain forward echelon crack system and two pre-existing cracks ($L_1 = L_2 = 20$ mm) (Figure 6(a)); inverse echelon cracks system and two pre-existing cracks ($L_1 = L_2 = 20$ mm) (Figure 6(b)); two parallel cracks and two pre-existing cracks ($L_1 = L_2 = 20$ mm) (Figure 6(c)); three parallel cracks and three pre-existing cracks ($L_1 = L_2 = L_3 = 20$ mm) (Figure 6(d)); crack system with barrier cracks and one pre-existing crack ($L = 20$ mm) and two pre-existing barrier cracks ($L_1 = L_2 = 20$ mm) (Figure 6(e)).

Several specimens with the same pre-existing flaw geometries were prepared to guarantee the reproducibility of the following experimental results presented. Table 1 shows the specimens containing different types of pre-existing flaws. The types of specimens are present as SC and CS for specimens with single pre-existing crack and the pre-existing crack systems; the flaws inclination angle, which is denoted by β, and followed by the sequential number of specimens. For example, SC15-2 represents the second, single pre-existing crack specimen with inclination angle $\beta = 15^\circ$. The specimens in italics mean that those are shown as the experimental results in Section 3.

2.2. Experimental Procedure. Generally, the underground rock mass exists in a state of compression stress, and the cracks propagate toward a direction parallel to the maximum compressive stress [20]. In the experimental process, the specimens were located in an appropriate position inside the two flat plates of the test machine and loaded by a diametric compressive force P. As shown in Figure 7, all samples were tested by an electronic universal testing machine with a capacity of 100 kN. The tests were carried out under displacement control conditions with a constant displacement rate of 0.05 mm/min. Monotonic loading was applied until the final crack propagation and coalescence form are reached.

3. Experimental Results

3.1. Crack Propagation Process of Pre-Cracked Specimens with a Single Crack. In the single pre-cracked specimens, most cracks are tensile cracks, but shear cracks may also be accompanied. Figure 8 shows the experimental results of crack propagation paths and the breakage process of specimens with different pre-existing inclination angles. The patterns are quite different for the specimen ($\beta = 0$) than those ($\beta = 15^\circ, 30^\circ, 45^\circ, 60^\circ, 75^\circ, 90^\circ$): wing cracks propagated in curved paths, starting their extension from the crack tips and continue their growth in a direction approximately parallel to compression direction. Meanwhile, crack propagation growth stopped at the release of the load. Figure 8(a) shows that there is no crack initiated from the tips of the pre-existing crack when $\beta = 0$. The wing cracks initiated from the middle of the pre-existing crack, and along the pre-crack perimeter, the tangential stresses are maximum like the uncracked specimen in a conventional Brazilian test. However, the cracks immediately propagated toward the edges of the specimens once they initiated.

Table 1: Specimens containing different types of pre-existing flaws.

Pre-existing flaw types	Tested specimens	Number of specimens
Single pre-existing crack	0	2 (SC0-1, *SC0-2*)
	15°	3 (SC15-1, *SC15-2*, SC15-3)
	30°	3 (SC30-1, *SC30-2*, SC30-3)
	45°	3 (SC30-1, SC30-2, *SC30-3*)
	60°	3 (*SC60-1*, SC60-2, SC60-3)
	75°	3 (SC75-1, *SC75-2*, SC75-3)
	90°	2 (*SC90-1*, SC90-2)
Pre-existing crack system	Forward echelon crack system	2 (*CSF-1*, CSF-2)
	Inverse echelon crack system	3 (CSI-1, *CSI-2*, CSI-3)
	Two parallel cracks	2 (*CSTw-1*, CSTw-2)
	Three parallel cracks	3 (*CSTh-1*, CSTh-2, CSTh-3)
	Crack system with barrier cracks	2 (CSB-1, *CSB-2*)
Total number		31

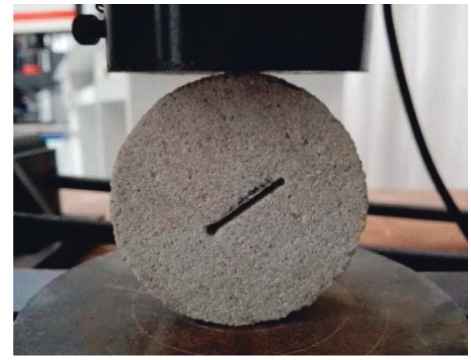

Figure 7: Load arrangements for the tested pre-cracked specimens.

3.2. Crack Propagation Process of Pre-Cracked Specimens with Crack Systems. In the specimens containing pre-existing crack systems, because of the propagation of wing cracks and secondary cracks, crack coalescence phenomenon occurred. Wing cracks propagated toward the direction of the maximum compressive stress. However, secondary cracks propagated and formed a corner with the opposite direction of pre-existing flaws. Even the cracks coalescence in the bridge areas may appear during the cracks' initiation and cracks propagation processes. Figure 9 illustrates the experimental results of crack propagation and coalescence in the specimens with different types of pre-existing crack systems.

The crack propagation and coalescence patterns are different depending on the types of crack systems. Figure 9(a) presents a specimen with the forward echelon crack system; cracks at the tips pre-existing crack systems were initiated in both directions and tip C of L_2 propagated to tip A of L_1 and coalesced at tip A. Crack from tip B of L_1 propagated to tip D of L_2 and coalesced at tip D. In the specimen containing inverse echelon crack system as shown in Figure 9(b), the crack at tip A of L_1 was initiated in an upward direction and the crack at tip D of L_2 was initiated in a downward direction steadily, and coalescence paths appeared between tips A and D. Figure 9(c) illustrates that cracks at the upward tips were initiated both toward upward

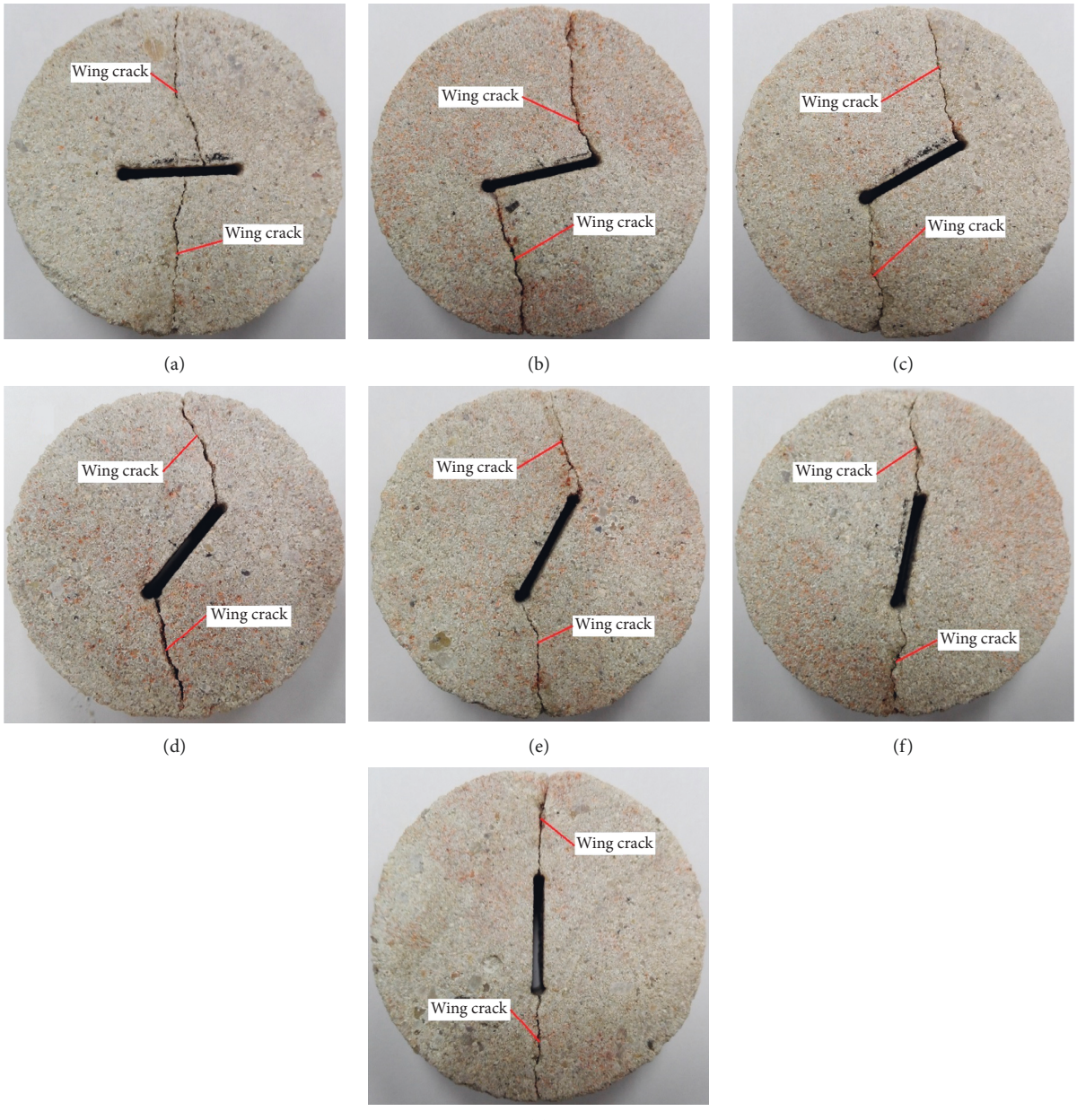

Figure 8: Experimental results of crack propagation paths in tested specimens with different pre-existing crack inclination angles: (a) $\beta = 0$, (b) $\beta = 15^{\circ}$, (c) $\beta = 30^{\circ}$, (d) $\beta = 45^{\circ}$, (e) $\beta = 60^{\circ}$, (f) $\beta = 75^{\circ}$, and (g) $\beta = 90^{\circ}$.

direction and crack at tip D were initiated towards downward direction and then coalescence path coalesced between tips B and D. As shown in Figure 9(d), there are three pre-existing cracks, L_1, L_2, and L_3, in this type specimen, and final cracks were only initiated at tips A and B of L_2 and propagated in upward and downward directions similarly like the propagation pattern in a single pre-cracked specimen with an inclination angle of $\beta = 60^{\circ}$. Figure 9(e) presents the crack system with barrier cracks L_1 and L_2; cracks at tips of pre-cracked flaws were initiated in both upward and downward directions, coalesced toward barrier cracks L_1 and L_2, and then one crack propagates from the left part of L_1 propagated upward direction and another in the middle of L_2 propagated downward direction. Interestingly, the crack propagation from AB was not blocked by the barrier cracks, and the crack propagation paths have changed after passed through the barrier cracks.

In the experiments, the wing cracks and secondary cracks interrelated with and propagated toward each other, which caused cracks coalescence in the bridge areas. Coalescence cracks originated from the tips of one pre-cracked flaw to another. Crack propagation patterns and characteristics in both single pre-cracked and pre-cracked crack system specimens are summarized in Table 2.

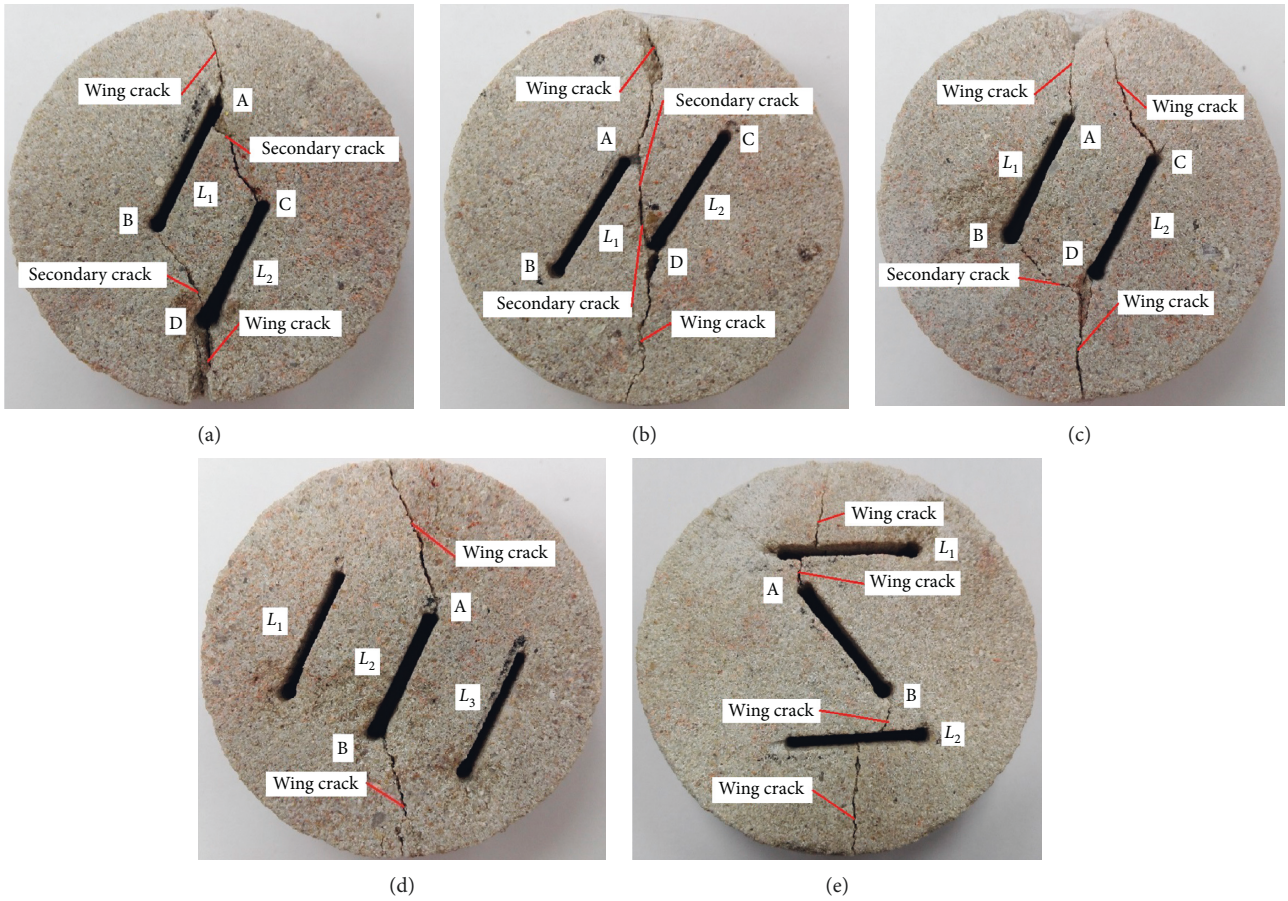

Figure 9: Experimental results of crack propagation and coalescence in specimens with different types of pre-existing crack systems. (a) Forward echelon crack system. (b) Inverse echelon crack system. (c) Two parallel cracks. (d) Three parallel cracks. (e) Crack system with barrier cracks.

Table 2: Crack propagation patterns and characteristics in pre-cracked specimens.

Flaw types in tested specimens	Patterns and characteristics
$\beta = 0$	1. Wing cracks were initiated from the middle portion of the pre-existing crack in the direction of the maximum compressive stress 2. Specimens fractured and split away due to the indirect tensile effect like uncracked specimens in conventional Brazilian tests 3. No secondary cracks
$\beta = 15^{\circ}$, 30°, 45°, 60°, 75°, and 90°	1. Wing cracks were initiated from the tips of the pre-existing crack in the direction parallel to the maximum compressive stress 2. No secondary cracks
Forward echelon crack system Inverse echelon crack system Two parallel cracks	1. Wing cracks were initiated from the tips of the pre-existing cracks in the direction of the maximum compressive stress 2. Secondary cracks were initiated after wing cracks 3. Cracks coalescence paths appeared between the two pre-existing cracks
Three parallel cracks	1. Wing cracks were initiated from the tips of the pre-existing crack in the direction parallel to the maximum compressive stress 2. No secondary cracks
Crack system with barrier cracks	1. Wing cracks were initiated from the tips of the pre-existing crack in the direction of the maximum compressive stress 2. Crack propagation of the pre-existing crack was not blocked by the barrier cracks 3. Crack propagation paths have changed after they passed through the barrier cracks

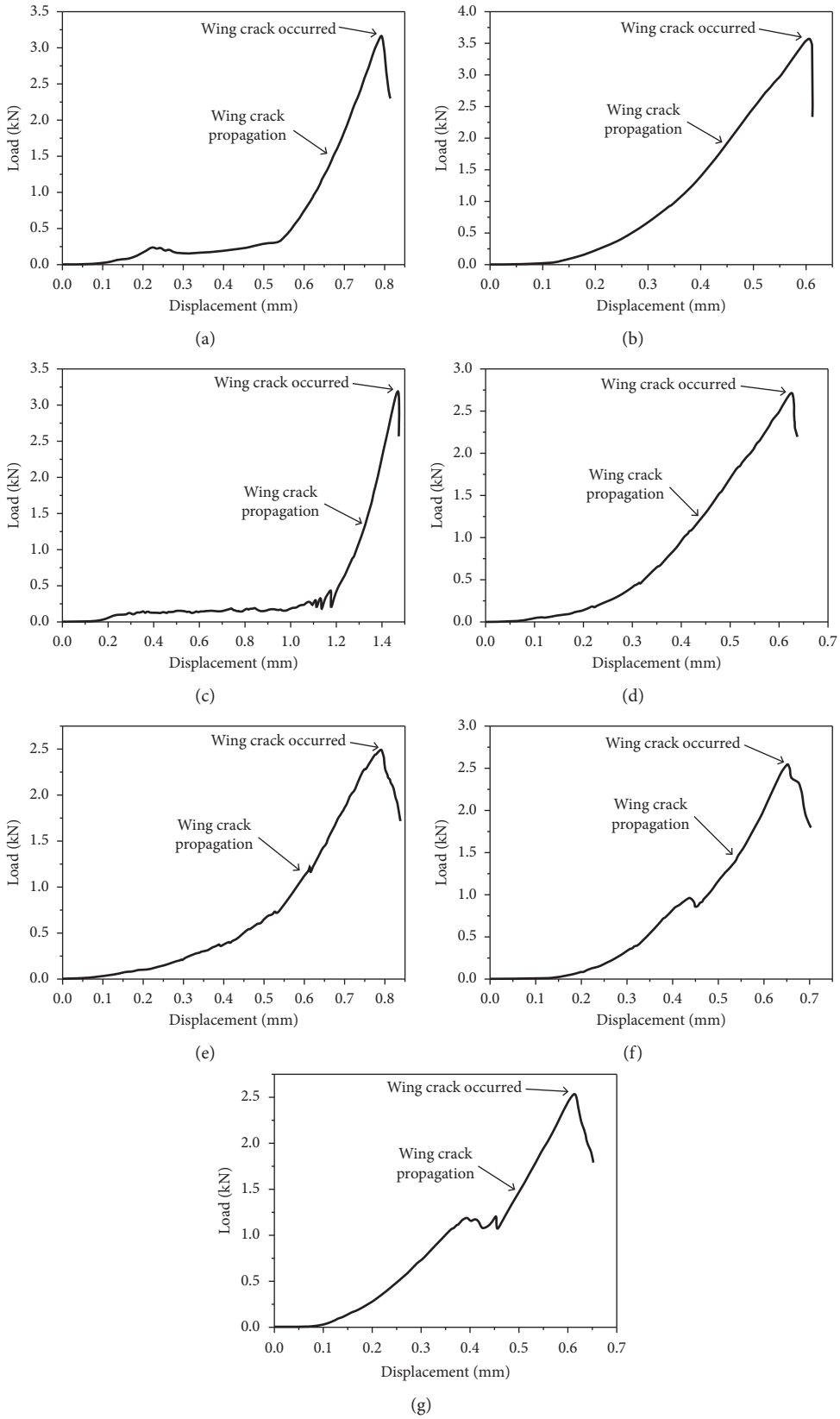

Figure 10: Load-displacement curves of the tested specimens with different pre-existing crack inclination angles: (a) $\beta = 0$, (b) $\beta = 15^{\circ}$, (c) $\beta = 30^{\circ}$, (d) $\beta = 45^{\circ}$, (e) $\beta = 60^{\circ}$, (f) $\beta = 75^{\circ}$, and (g) $\beta = 90^{\circ}$.

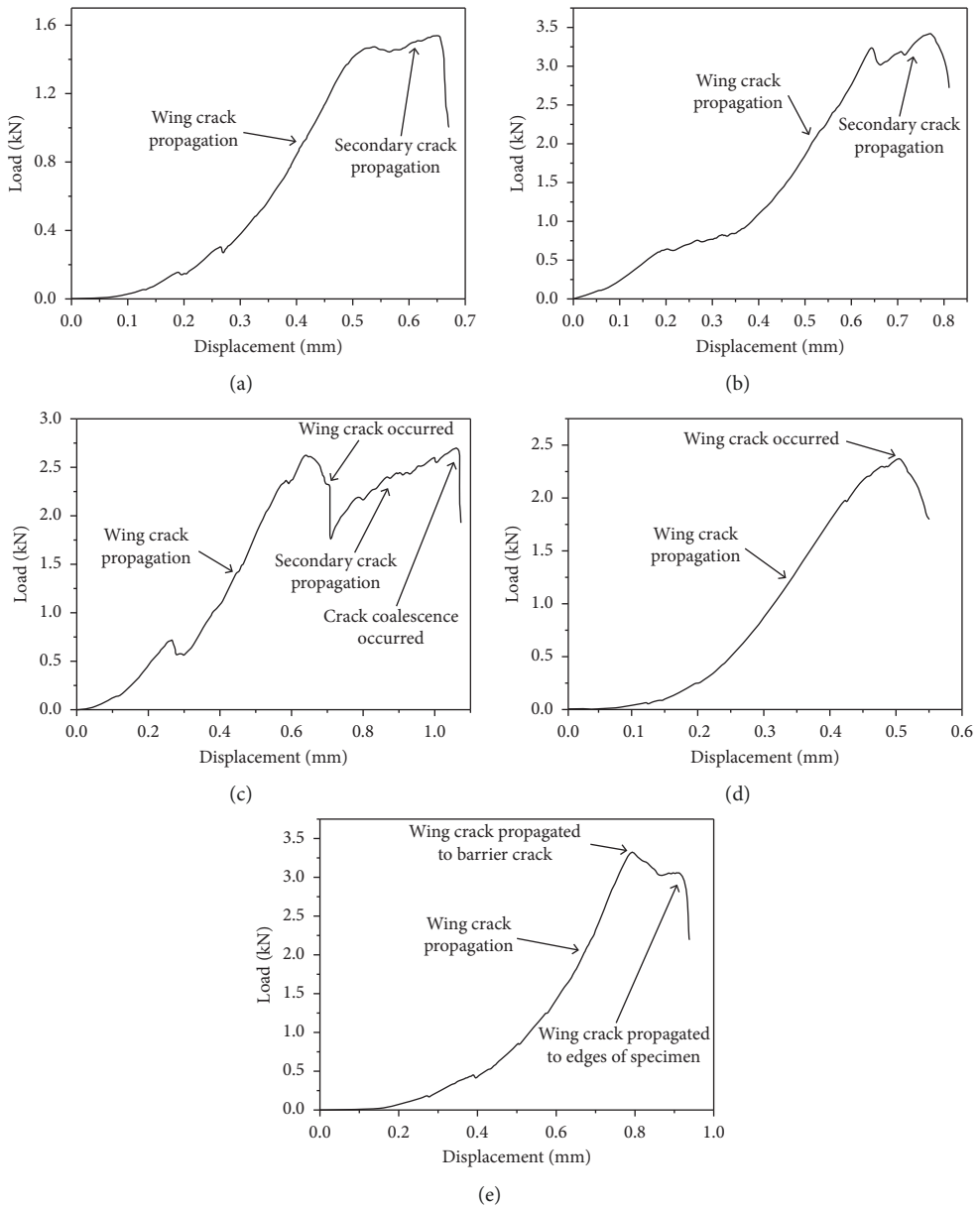

Figure 11: Load-displacement curves of the specimens with different types of crack systems. (a) Forward echelon crack system. (b) Inverse echelon crack system. (c) Two parallel cracks. (d) Three parallel cracks. (e) Crack system with barrier cracks.

4. Discussion

In this section, we discuss the experimental data. Figure 10 indicates the load-displacement curves of the pre-cracked specimens with different inclination angles. It can be seen that pre-cracked specimens fractured suddenly from the crack tips in a typical brittle manner after the load-displacement curves reach its peak. That means the specimens began to fracture when the wing cracks extended to a critical length of the specimens' edges and the specimens were split into two nearly same halves.

Typical load-displacement curves for the specimens containing pre-cracked crack systems are shown in Figure 11. Based on Figures 11(a), 11(b),11(c), and 11(e), one of the noticeable characteristics is the decrease in loading after the wing cracks appeared. It means that the wing cracks propagated to the edges from tips of the pre-existing cracks after the first peak value in the load-displacement curves. Then, the secondary cracks began to propagate. After the secondary peak value in the load-displacement curves, those specimens began to fail, and cracks coalescence occurred. In other words, the cracks coalescence appeared mainly caused by the wing cracks or their propagation and the combined effects of wing cracks and secondary cracks. In Figure 11(d), the specimen with three parallel cracks, wing crack extends to the specimen's edges and the specimen splits into two same halves. The fracture and failure patterns are similar to those with single pre-cracked specimens.

5. Conclusions

Crack initiation, propagation, and coalescence are a rather difficult and complicated process. It is not only determined by the material but also dependent on the geometries of the pre-existing flaws. In this paper, BD specimens with single pre-existing crack and the pre-existing crack system were experimentally investigated, and the effects of fracturing on the failure load of the tested specimens have been discussed. The following conclusions can be drawn from the results presented above:

(1) Two type cracks were observed: wing cracks and secondary cracks. Both mainly initiated from tips of the pre-existing flaws and propagated in a stable manner. Wing cracks appear at the first stage of loads applied and propagate toward the compression direction, and then the secondary cracks initiate afterward. This can lead to crack coalescence with breakage processes. According to the different geometries of pre-existing flaws, the tested specimens experienced wing crack propagation failure or crack coalescence failure.

(2) In this experimental work, crack coalescence appears by the linkage of two pre-existing flaws through combinations of the wing and/or secondary cracks. According to the different geometries of pre-existing flaws, crack coalescence patterns are different. Cracks propagation and coalescence were not blocked by the barrier cracks, and the crack propagation paths have changed after they passed through the barrier cracks.

(3) From the results, the pre-existing flaws or fractures play a significant role in the overall integrity that can help to analyze the stability of rock masses and rock structures.

Data Availability

The data used to support the findings of this study are available from the corresponding author upon request.

Conflicts of Interest

The authors declare that they have no conflicts of interest.

Acknowledgments

The research described in this paper was financially supported by the National Natural Science Foundation of China (Nos. 11672101, 11132003, and 11372099), National Key Technologies Research & Development Program (No. 2017YFC1502600), Natural Science Foundation of Jiangsu Province (No. BK20151493), Postgraduate Research & Practice Innovation Program of Jiangsu Province (No. KYLX16_0700), and Fundamental Research Funds for the Central Universities (No. 2016B45214). The authors wish to acknowledge Prof. Florin Bobaru for polishing the manuscript.

References

[1] A. Bobet and H. H. Einstein, "Fracture coalescence in rock-type materials under uniaxial and biaxial compression," *International Journal of Rock Mechanics and Mining Sciences*, vol. 35, no. 7, pp. 863–888, 1998.

[2] E. Hoek and C. D. Martin, "Fracture initiation and propagation in intact rock—a review," *Journal of Rock Mechanics and Geotechnical Engineering*, vol. 6, no. 4, pp. 287–300, 2014.

[3] D. Huang, D. Gu, C. Yang, R. Huang, and G. Fu, "Investigation on mechanical behaviors of sandstone with two pre-existing flaws under triaxial compression," *Rock Mechanics and Rock Engineering*, vol. 49, no. 2, pp. 375–399, 2015.

[4] M. D. Kuruppu, Y. Obara, M. R. Ayatollahi, K. P. Chong, and T. Funatsu, "ISRM-suggested method for determining the mode I static fracture toughness using semi-circular bend specimen," *Rock Mechanics and Rock Engineering*, vol. 47, no. 1, pp. 267–274, 2013.

[5] M. D. Kuruppu, "Fracture toughness measurement using chevron notched semi-circular bend specimen," *International Journal of Fracture*, vol. 86, no. 4, pp. 33–38, 1997.

[6] A. M. Shiryaev and A. M. Kotkis, "Methods for determining fracture toughness of brittle porous materials," *Industrial Laboratory*, vol. 48, no. 9, pp. 917-918, 1983.

[7] M. Thiercelin and J. C. Roegiers, "Fracture toughness determination with the modified ring test," in *Proceedings of the international symposium on engineering in complex rock formations*, pp. 1–8, Beijing, China, November 1986.

[8] W. F. Brace and E. G. Bombolakis, "A note on brittle crack growth in compression," *Journal of Geophysical Research*, vol. 68, no. 12, pp. 3709–3713, 2012.

[9] A. Bobet, "The initiation of secondary cracks in compression," *Engineering Fracture Mechanics*, vol. 66, no. 2, pp. 187–219, 2000.

[10] N. A. Al-Shayea, "Crack propagation trajectories for rocks under mixed mode I-II fracture," *Engineering Geology*, vol. 81, no. 1, pp. 84–97, 2005.

[11] H. Q. Li and L. N. Y. Wong, "Initiation and propagation of tensile wing cracks and horsetail cracks from a pre-existing flaw under compression (ARMA 11–341)," in *Proceedings of 45th US Rock Mechanics Geo-Mechanics Symposium*, San Francisco, CA, USA, June 2011.

[12] H. Li and L. N. Y. Wong, "Influence of flaw inclination angle and loading condition on crack initiation and propagation," *International Journal of Solids and Structures*, vol. 49, no. 18, pp. 2482–2499, 2012.

[13] S. Q. Yang, H. W. Jing, and S. Y. Wang, "Experimental investigation on the strength, deformability, failure behavior and acoustic emission locations of red sandstone under triaxial compression," *Rock Mechanics and Rock Engineering*, vol. 45, no. 4, pp. 583–606, 2012.

[14] S. Q. Yang, Y. H. Huang, W. L. Tian, and J. B. Zhu, "An experimental investigation on strength, deformation and crack evolution behavior of sandstone containing two oval flaws under uniaxial compression," *Engineering Geology*, vol. 217, pp. 35–48, 2017.

[15] X. Zhuang, J. Chun, and H. Zhu, "A comparative study on unfilled and filled crack propagation for rock-like brittle material," *Theoretical and Applied Fracture Mechanics*, vol. 72, pp. 110–120, 2014.

[16] X. P. Zhang, Q. Liu, S. Wu, and X. Tang, "Crack coalescence between two non-parallel flaws in rock-like material under

uniaxial compression," *Engineering Geology*, vol. 199, pp. 74–90, 2015.

[17] C. H. Park, "Coalescence of frictional fracture in rock materials," Ph. D. thesis, Purdue University, West Lafayette, Indiana, 2008.

[18] C. H. Park and A. Bobet, "Crack initiation, propagation and coalescence from frictional flaws in uniaxial compression," *Engineering Fracture Mechanics*, vol. 77, no. 14, pp. 2727–2748, 2010.

[19] R. P. Janeiro and H. H. Einstein, "Experimental study of the cracking behavior of specimens containing inclusions (under uniaxial compression)," *International Journal of Fracture*, vol. 164, no. 1, pp. 83–102, 2010.

[20] P. Cao, T. Liu, C. Pu, and H. Lin, "Crack propagation and coalescence of brittle rock-like specimens with pre-existing cracks in compression," *Engineering Geology*, vol. 187, pp. 113–121, 2015.

[21] L. N. Y. Wong and H. H. Einstein, "Crack coalescence in molded gypsum and carrara marble: part 1. Macroscopic observations and interpretation," *Rock Mechanics and Rock Engineering*, vol. 42, no. 3, pp. 475–511, 2008.

[22] L. N. Y. Wong and H. H. Einstein, "Crack coalescence in molded gypsum and carrara marble: part 2. Microscopic observations and interpretation," *Rock Mechanics and Rock Engineering*, vol. 42, no. 3, pp. 513–545, 2008.

[23] R. H. C. Wong, K. T. Chau, C. A. Tang, and P. Lin, "Analysis of crack coalescence in rock-like materials containing three flaws-part I: experimental approach," *International Journal of Rock Mechanics and Mining Sciences*, vol. 38, no. 7, pp. 909–924, 2001.

[24] R. H. C. Wong, C. A. Tang, K. T. Chau, and P. Lin, "Splitting failure in brittle rocks containing pre-existing flaws under uniaxial compression," *Engineering Fracture Mechanics*, vol. 69, no. 17, pp. 1853–1871, 2002.

[25] M. Sagong and A. Bobet, "Coalescence of multiple flaws in a rock-model material in uniaxial compression," *International Journal of Rock Mechanics and Mining Sciences*, vol. 39, no. 2, pp. 229–241, 2002.

[26] Y. P. Li, L. Z. Chen, and Y. H. Wang, "Experimental research on pre-cracked marble under compression," *International Journal of Solids and Structures*, vol. 42, no. 9-10, pp. 2505–2516, 2005.

[27] Q. Lin, A. Fakhimi, M. Haggerty, and J. F. Labuz, "Initiation of tensile and mixed-mode fracture in sandstone," *International Journal of Rock Mechanics and Mining Sciences*, vol. 46, no. 3, pp. 489–497, 2009.

[28] H. Lee and S. Jeon, "An experimental and numerical study of fracture coalescence in pre-cracked specimens under uniaxial compression," *International Journal of Solids and Structures*, vol. 48, no. 6, pp. 979–999, 2011.

[29] S. P. Morgan, C. A. Johnson, and H. H. Einstein, "Cracking processes in Barre granite: fracture process zones and crack coalescence," *International Journal of Fracture*, vol. 180, no. 2, pp. 177–204, 2013.

[30] P. Yin, R. H. C. Wong, and K. T. Chau, "Coalescence of two parallel pre-existing surface cracks in granite," *International Journal of Rock Mechanics and Mining Sciences*, vol. 68, pp. 66–84, 2014.

[31] X. P. Zhou, H. Cheng, and Y. F. Feng, "An experimental study of crack coalescence behavior in rock-like materials containing multiple flaws under uniaxial compression," *Rock Mechanics and Rock Engineering*, vol. 47, no. 6, pp. 1961–1986, 2014.

[32] H. Cheng, X. P. Zhou, J. Zhu, and Q. H. Qian, "The effects of crack opening on crack initiation, propagation and coalescence behavior in rock-like materials under uniaxial compression," *Rock Mechanics and Rock Engineering*, vol. 49, no. 9, pp. 3841–3494, 2016.

[33] Y. Zhao, L. Zhang, W. Wang, C. Pu, W. Wan, and J. Tang, "Cracking and stress-strain behavior of rock-like material containing two flaws under uniaxial compression," *Rock Mechanics and Rock Engineering*, vol. 49, no. 7, pp. 2665–2687, 2016.

[34] M. R. M. Aliha and A. Bahmani, "Rock fracture toughness study under mixed mode I/III loading," *Rock Mechanics and Rock Engineering*, vol. 50, no. 7, pp. 1739–1751, 2017.

[35] Z. P. Bazant and M. T. Kazemi, "Determination of fracture energy, process zone length and brittleness number from size effect, with application to rock and concrete," *International Journal of Fracture*, vol. 44, no. 2, pp. 111–131, 1990.